Molecular Dynamics Simulations of the Charge-Induced Unfolding and Refolding of Unsolvated Cytochrome *c*

Yi Mao, Mark A. Ratner,* and Martin F. Jarrold*

Department of Chemistry, Northwestern University, 2145 Sheridan Road, Evanston, Illinois 60208

Received: March 30, 1999; In Final Form: August 30, 1999

The charge-induced unfolding and refolding of unsolvated cytochrome *c* have been studied by molecular dynamics (MD) simulations. Simulations were performed for protonated charge states between +3 and +19. The charge-induced unfolding of cytochrome *c* in the gas phase has previously been examined by ion mobility measurements. The main features of the experimental results are reproduced by the MD simulations reported here. The simulations provide insight into how the energy landscape changes with charge, and into the nature of the unfolded conformations of the higher charge states. Experiments have shown that unsolvated cytochrome *c* refolds when the charge is reduced. MD simulations of this refolding process were also performed. When the charge is reduced, the protein ions collapse, but they became trapped in random loop conformations with little secondary structure.

Introduction

The pH dependence of protein stability in solution has been extensively investigated, both experimentally and theoretically.[1−8] It has been argued that the driving force for acid denaturation is the change in the electrostatic free energy of the folded and unfolded protein at low pH, which includes contributions from the shift in the pK_a values of the ionizable groups and from electrostatic interactions.[5] Unsolvated proteins can be produced in the gas phase in a variety of protonated charge states, and the charge-induced unfolding of an unsolvated protein is the gas-phase analogue of acid denaturation in solution. Ion mobility experiments have been used to examine the unfolding of proteins in vacuo as a function of charge.[9−17] Mobility measurements provide a measure of the average collision cross section of a protein, which is related to its conformation.[18] The conformations of gas-phase cytochrome *c* ions have also been examined in a series of H/D exchange studies.[19−21] One advantage of studying proteins in the gas phase is that the charge state can be defined, while in solution at a specific pH there is a distribution of charge states present.[5] Here, we report folding studies for cytochrome *c* and compare the molecular dynamics (MD) results to the results of gas phase ion mobility measurements. Reimann and collaborators have similarly used MD simulations to examine the unfolding of highly charged lysozyme in vacuo.[22]

The acid denaturation of cytochrome *c* has been studied since the 1940s,[23−26] and the folding of cytochrome *c* has been studied as a model system for several decades.[27,28,29] The term molten globule was first used to describe an intermediate observed in the acid denaturation of cytochrome *c*.[30] In vacuo, ion mobility measurements show that cytochrome *c* ions unfold as the charge increases. The MD simulations described here were performed to see if they could reproduce the unfolding transitions observed in the experiments and to provide some information about the nature of the unfolded conformations of the higher charge states.

Theoretical Methods

The MD simulations were performed with the Macsimus molecular modeling package[31] with CHARMM-like potentials[32] (21.3 parameter set). The Coulomb potentials were not truncated because this is unnecessary for the isolated protein ions studied here. Bond lengths were constrained by SHAKE[33] and CH, CH_2, and CH_3 groups were treated as united atoms. The time step was 1 fs, and the temperature was kept at 300 K by rescaling the kinetic energy every 0.1 ps. Simulations were performed for the +3, +5, +7, +9, +11, +13,+15, +17, and +19 protonated charge states of cytochrome *c*. Cytochrome *c* has many basic sites that can be protonated, and there is an enormous number of ways of distributing the protons among the sites.[34] Ten charge permutations were chosen for each charge state using a sampling method described elsewhere.[14] Although the selected permutations are believed to be in the low energy regime, this sample is almost certainly too small to identify the lowest energy charge permutation. However, the sample is large enough to examine how the location of the protons affects the results. To simulate the gas phase, all residues were neutral except for those that were specifically protonated to account for the charge. Except in the refolding studies, the initial conformation was the minimized crystal structure[35] with modified protonation sites. Crystal waters were removed. The simulations were run until no further unfolding or refolding was observed for at least 240 ps. The simulation times ranged from 480 ps (for the high charge states) to several nanoseconds. Average energies and cross sections (for comparison with the results of the ion mobility measurements) were derived from the final 240 ps. The cross sections were calculated by the exact hard spheres scattering model,[36] which for large protein ions provides results that are close to those obtained by the more accurate trajectory method.[37]

Unfolding

Cross sections derived from the MD simulations are compared with the measured cross sections in Figure 1. The experimental results depend on the conditions. For cytochrome *c* electrosprayed from an unacidified aqueous solution, cross sections were measured for the +6 to +10 charge states (shown by open triangles in the figure).[13] For an acidified solution, cross sections were measured for the +7 to +19 charge states (shown by open

10.1021/jp991093d CCC: $18.00
Published on Web 10/22/1999

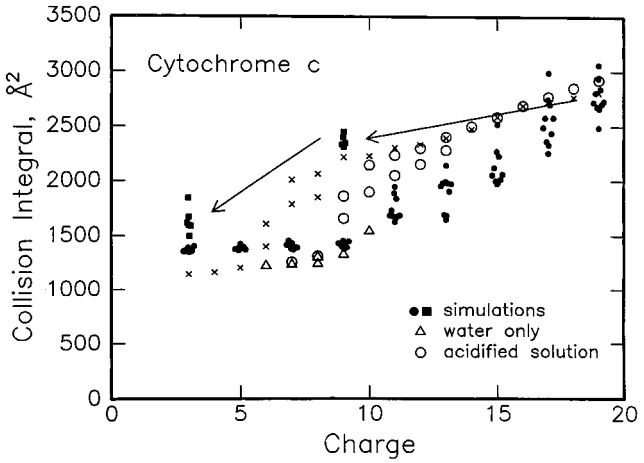

Figure 1. Cross sections measured for the +3 to +19 charge states of cytochrome *c* and cross sections determined from the MD simulations for the +3, +5, +7, +9, +11, +13, +15, +17, and +19 charge states. The cross sections derived from the simulations are indicated by the filled points. The filled circles are for simulations started from the crystal structure, while the filled squares represent the results of refolding studies (as shown by the arrows). The open triangles are cross sections measured with an unacidified aqueous solution, the open circles were measured with an acidified solution, and the crosses were measured for collisionally heated ions (where the nature of the solution is unimportant).

circles).[13] In addition, cross sections are shown in Figure 1 for collisionally heated +3 to +19 charge states (shown by crosses).[12] The low charge state ions were prepared by proton transfer reactions from higher charge states. When the ions are collisionally heated, the results do not depend on the solution conditions. Together, these results show that an unfolding transition occurs for charge states between +6 to +10 (depending on the conditions) and then the cross sections gradually increase with increasing charge. The unfolding transition occurs for lower charge states when the ions are collisionally heated.

Cross sections derived from the MD simulations are shown as filled circles in Figure 1. For the +3 to +9 charge states, the cross sections are similar to that calculated for neutral cytochrome *c*. The calculated cross sections increase slightly with increasing charge. The main features of the secondary and tertiary structure of the native conformation (the crystal structure) are preserved in the simulations for the +3 to +9 charge states. The only substantial deviations from the native conformation are some disorder in the loop regions and that the Met80−heme iron bond is replaced by an Fe−O bond. The calculated cross sections are slightly larger than the measured cross sections (except those for the collisionally heated ions). The measured cross sections indicate a conformation that is more compact than the crystal structure. However, the contraction that occurs on removing the solvent is not reproduced by the simulations, presumably because of the way the force field is parametrized.[14]

The +11 charge state is the lowest charge state to be significantly unfolded in these room temperature simulations. The difference between the +9 and +11 charge states is that the terminal helices have disengaged, opening up the hydrophobic core. Figure 2 shows typical conformations from the simulations. The range of cross sections determined for the +11 charge states (see Figure 1) reflects the dispersion in the amount of unfolding that occurs for the different charge permutations. The N-terminus helix is disrupted in the two most unfolded charge permutations. Ions electrosprayed from an unacidified aqueous solution (open triangles in Figure 1) provide the best comparison with the simulations because these ions start in the native conformation in solution. For these ions, the first indication of unfolding occurs for the +8 charge state where two slightly different conformations were resolved. However, the +10 charge state is the first to show the protein in a substantially unfolded conformation. This is in good agreement with the simulations, where significant unfolding occurs between the +9 and +11 charge states.

For the +11 to +19 charge states, the protein becomes progressively more unfolded. There is considerable overlap between the cross sections calculated for nearby charge states because of the distribution of conformations from the different charge permutations. Moving from the +11 to +15 charge states, the N-terminus helix gradually drifts away from the middle and C-terminus helices. These helices remain in contact (see Figure 2) and keep the C end of the protein compact. Starting at around the +15 charge state, the middle and C-terminus helices begin to separate. The middle and C-terminus helices are disrupted at around the +17 charge state. Further unfolding of the +17 and +19 charge states is achieved by straightening out the loops and disrupting the remaining helices. In some simulations, the N-terminus helix persists even for the +19 charge state. For the low charge states, up to +9, the Met80 ligand to the heme iron is replaced by an oxygen atom. Starting at +11, the iron gradually switches to five coordinate with His18 as the only axial ligand.

Cross sections derived from the simulations for the +11, +13, and +15 charge states are significantly smaller than the measured cross sections (see Figure 1). However, for these charge states, measurements could not be performed with an unacidified aqueous solution. The measured cross sections that are available for these charge states were derived from either acidified solutions or from experiments on collisionally heated ions. Collisional heating unfolds the ions in the gas phase and cytochrome *c* is denatured in the acidified solutions that were used, so the comparison between the simulations and experiment for these charge states is not straightforward. It is possible that, if the simulations were run for a much longer time, further unfolding would occur and the agreement with the experiments would improve.

For the high charge states, +17 and +19, there is closer agreement between cross sections derived from the simulations and from the experiments. As for the +11 to +15 charge states, the measured cross sections for +17 and +19 charge states were derived from either acidified solutions or from experiments on collisionally heated ions. However, this is apparently not as important for these high charge states, presumably because the electrostatic interactions are so strong. In the simulations, the +19 charge states are almost completely unfolded into extended strings. Since the calculated cross sections for these conformations are in reasonable agreement with the measured ones, the conformations sampled in the experiments must be almost completely unfolded like the ones in the simulations.

Figure 3 shows plots of the electrostatic energy and van der Waals energy for the first 30 ps of one of the simulations for the +19 charge state. Unfolding leads to a more negative electrostatic energy and a more positive van der Waals energy. The change in the electrostatic energy outweighs the loss of favorable van der Waals contacts. The electrostatic interactions include both repulsive and attractive interactions. The latter includes hydrogen bonds formed between protonated residues and nearby oxygen atoms, which leads to the formation of a "solvation" shell. The "solvation" shells around the protonation sites contain from one to eight carbonyl or side chain oxygens,

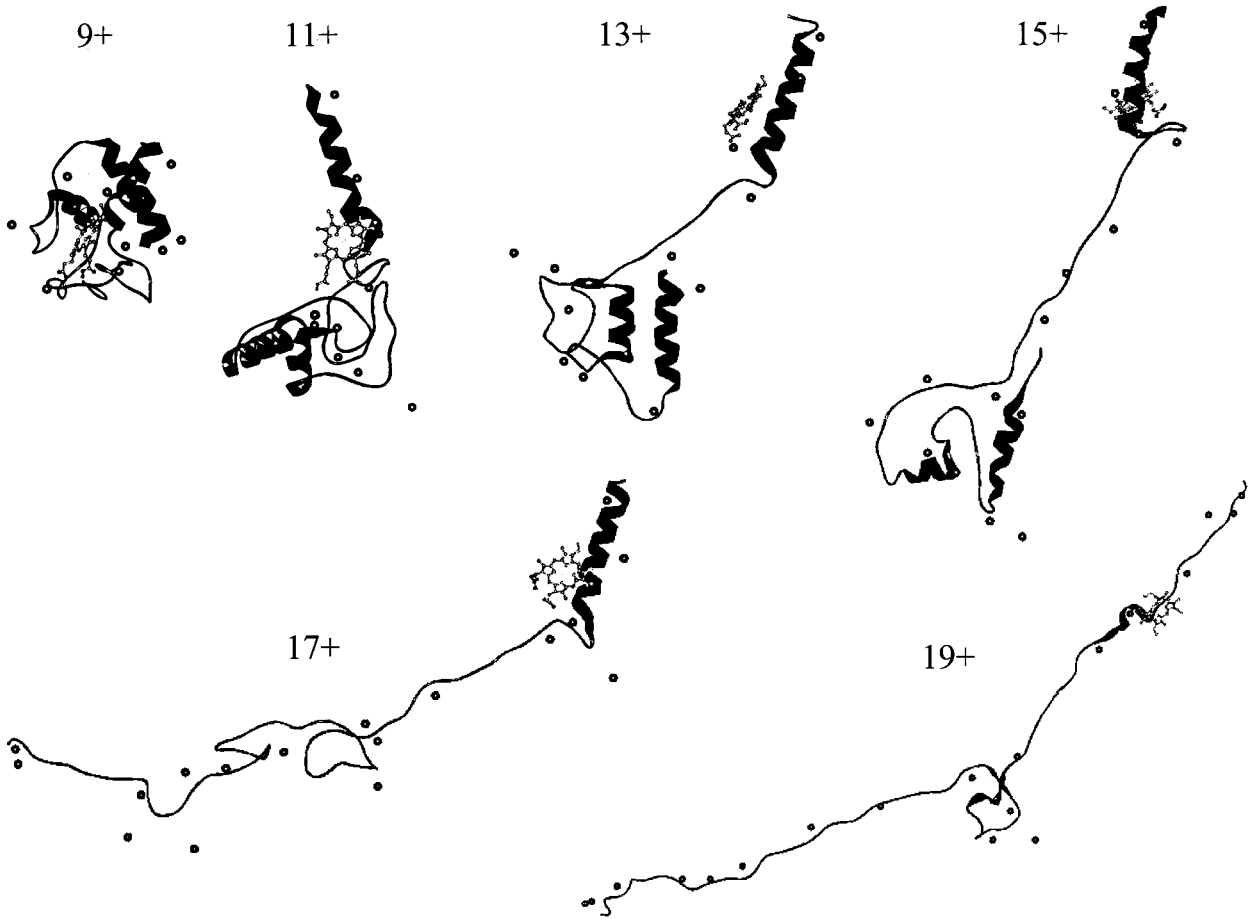

Figure 2. Representative structures from the simulations for the +9, +11,+13, +15, +17, and +19 charge states. For the unfolded conformations, the N-termini are at the top of the page. The circles show the locations of the protons.

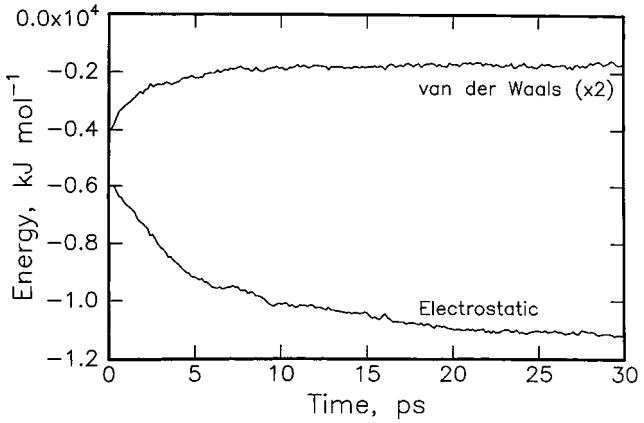

Figure 3. Plot of the electrostatic energy and van der Waals energy against time for one of the +19 charge states. Results are shown for the first 30 ps of the MD run.

depending on steric effects and the overall conformation. When the protein unfolds, the average number of oxygen atoms in the solvation shells drops. But even for the +19 charge states, a local solvation shell exists for all of the protonation sites. Overall protonation leads to increase in the electrostatic energy, and the average electrostatic energy rises monotonically as a function of the charge.

Refolding

The refolding of cytochrome *c* in the gas phase has been studied by H/D exchange[21] and by ion mobility experiments.[10] In these experiments, lower charge states were produced by proton transfer reactions from higher charge states. In the mobility studies, compact conformations were observed for the lower charge states even when they were produced from unfolded higher charge states. So cytochrome *c* refolds in the gas phase. To simulate the refolding observed in the experiments, unfolded conformations generated in the simulations for higher charge states were used as the starting conformations for simulations of lower charge states. Six refolding trajectories were generated by starting from six of the charge permutations of the +19 charge state and removing 10 protons. The resulting refolded +9 charge states were then used as the starting point for refolding studies of the +3 charge states. The refolded +9 charge states (see Figure 4) have conformations that are quite similar to those of the original +19 charge states. They are slightly more compact (by up to 500 Å^2 in terms of the cross section). Refolding occurs mainly by the formation of small random loops. The refolded +9 conformations are much less compact than the +9 conformations generated by starting the simulations from the crystal structure. However, the energies of the refolded +9 conformations are similar to the energies of the compact +9 conformations. This demonstrates the broad nature of the energy landscape of the intermediate charge states. We observed similar behavior in folded and extended cytochrome *c* +7 at 600 K. The calculated cross sections for the refolded +9 charge states are quite close to cross sections measured for collisionally heated ions, suggesting that the collisionally heated ions have similar conformations to the refolded ones. The refolded +3 charge states have more compact structures (see Figure 4), but there is no evidence for the formation of ordered structures. The cross sections are 100−

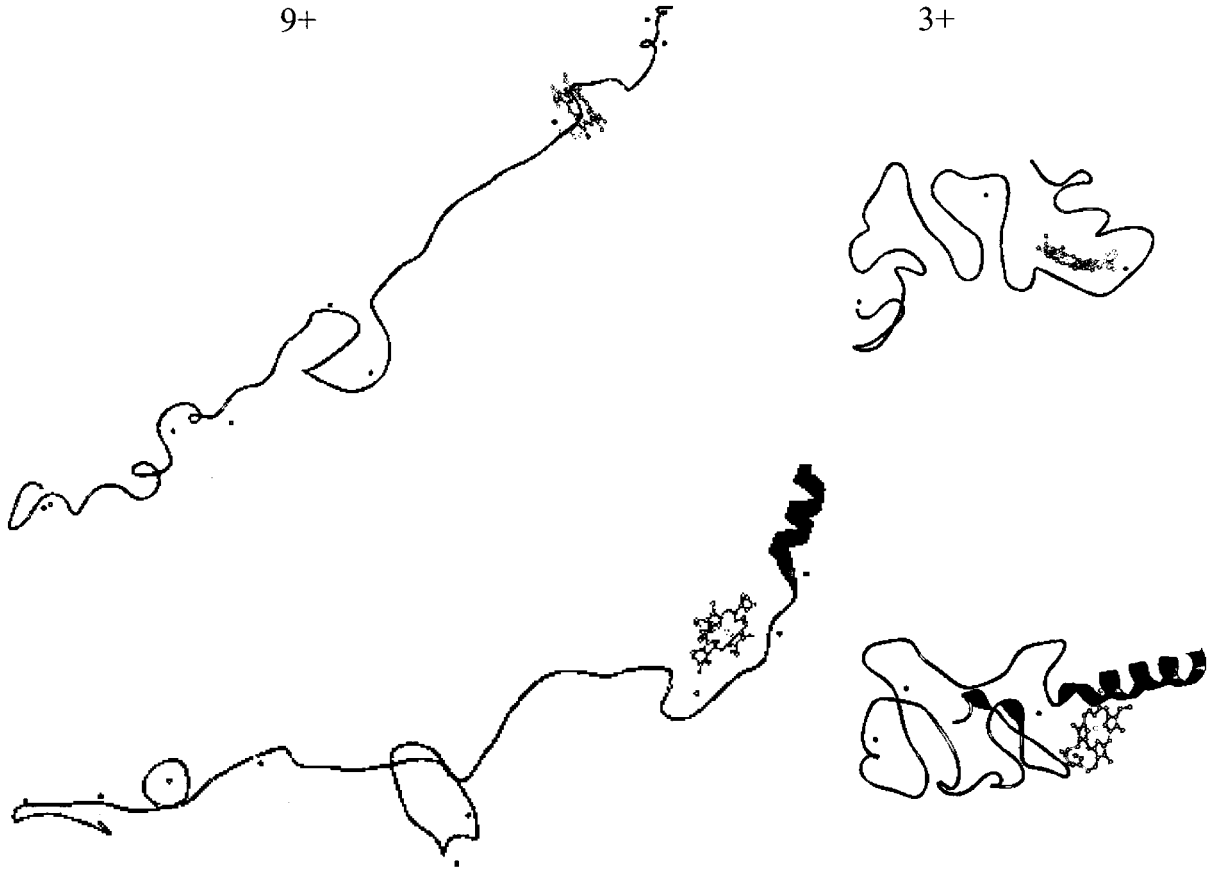

Figure 4. Representative refolded conformations of the +9 and +3 charge states. The +9 charge states were started from unfolded +19 conformations, and the +3 charge states were started from the refolded +9 charge states. The circles show the locations of the protons.

500 Å^2 larger than those for the nativelike +3 charge states and the energies are 300−500 kJ mol^{-1} higher. For the +3 charge state, electrostatic repulsion is small and the folded conformation is favored energetically. The re-emergence of secondary structure in the refolding simulations is rare. In some cases, the N-terminal helix reforms. When this happens, it usually occurs at the very beginning of simulation. Refolding of the C-terminal helix was not observed on the time scale of simulations, instead a loop usually forms at the C-terminus.

The random collapsed conformations generated in the simulations for the +3 charge states may have a lot in common with the conformations generated in the initial collapse that occurs in the experiments.[10] In the experiments, the most compact conformations are not produced by just stripping off the protons. The ions must be collisionally heated to generate conformations that are as compact as the native form. The failure of the simulations to refold cytochrome *c* is a manifestation of the folding problem. The time scale of simulations is many orders of magnitude shorter than expected for the protein to refold properly, so it is not surprising that the simulations do not lead to ordered structures. The refolding simulations lead to collapsed conformations with random loops and little secondary structure. Similar nonspecific collapse was found by Alonso and Daggett in MD simulations of ubiquitin refolding in solution.[38] It has been suggested that the slow step in the folding of cytochrome *c* is the reorganization of misfolded structures trapped during the initial collapse.[25]

Conclusions

Molecular dynamics simulations have been used to examine the charge-induced unfolding of cytochrome *c*. Overall, the simulations reproduce the main features of the experimental results. In particular, the simulations predict the onset of the charge-induced unfolding at around the +10 charge state. This suggests that there is a good balance between the electrostatic repulsions and the attractive interactions in the force field. In the simulations, the high charge states, +17 and +19, are almost completely unfolded into extended structures. The agreement between the measured and calculated cross sections for these charge states suggests that they indeed have these extended structures.

When 10 protons are removed from the +19 charge states, the resulting +9 collapses slightly by forming some random loops. The cross section for this refolded +9 is quite close to cross sections measured for collisionally heated +9 ions, suggesting that the collisionally heated ions have similar extended structures that are significantly larger than the refolded, ambient temperature +9. The energies of the refolded +9 and the compact +9 generated from the crystal structure are quite close. This demonstrates how electrostatic repulsion broadens out the energy landscape for the intermediate charge states, which explains why compact and folded conformations are observed for these charge states depending on the experimental conditions. The collapsed +3 charge states adopt compact conformations because electrostatic repulsions are small and the folded conformation is favored energetically. However, as in the experiments, the refolded ions do not achieve the most compact conformations in the initial collapse because they become trapped in misfolded structures.

Acknowledgment. We thank Jiri Kolafa for helpful advice and for the use of his Macsimus molecular modeling package. We gratefully acknowledge support from the DOE/LBL Ad-

vanced Battery Program, the National Science Foundation, and the Petroleum Research Fund administered by the American Chemical Society.

References and Notes

(1) Linderstrøm-Lang, K. C. R. *Trav. Lab. Carlsberg* **1924**, *15*, 1.
(2) Tanford, C.; Kirkwood, J. G. *J. Am. Chem. Soc.* **1957**, *79*, 5333.
(3) Tanford, C.; Roxby, R. *Biochemistry* **1972**, *11*, 2192.
(4) Bashford, D.; Karplus, M. *Biochemistry* **1990**, *29*, 10219.
(5) Schaefer, M.; Sommer, M.; Karplus, M. *J. Phys. Chem.* **1997**, *101*, 1663.
(6) Sternberg, M. J. E.; Hayes, F. R. F.; Russell, A. J. Thomas, P. G.; Fersht, A. R. *Nature* **1987**, *330*, 84.
(7) Warshel, A.; Russell, S. *Q. Rev. Biophys.* **1984**, *17*, 283.
(8) Sharp, K. A.; Honig, B. *Annu. Rev. Biophys. Chem.* **1990**, *19*, 301.
(9) Clemmer, D. E.; Hudgins, R. R.; Jarrold, M. F. *J. Am. Chem. Soc.* **1995**, *117*, 10141.
(10) Shelimov, K. B.; Jarrold, M. F. *J. Am. Chem. Soc.* **1996**, *118*, 10313.
(11) Shelimov, K. B.; Jarrold, M. F. *J. Am. Chem. Soc.* **1997**, *119*, 2987.
(12) Shelimov, K. B.; Clemmer, D. E.; Hudgins, R. R.; Jarrold, M. F. *J. Am. Chem. Soc.* **1997**, *119*, 2240.
(13) Hudgins, R. R.; Woenckhaus, J.; Jarrold, M. F. *Int J. Mass Spectrom. Ion Processes* **1997**, *165*, 497.
(14) Mao, Y.; Woenckhaus, J.; Kolafa, J.; Ratner, M. A.; Jarrold, M. F. *J. Am. Chem. Soc.*, in press.
(15) Valentine, S. J.; Clemmer, D. E. *J. Am. Chem. Soc.* **1997**, *119*, 3558.
(16) Valentine, S. J.; Anderson, J. G.; Ellington, A. D.; Clemmer, D. E. *J. Phys. Chem. B* **1997**, *101*, 3891.
(17) Valentine, S. J.; Counterman, A. E.; Clemmer, D. E. *J. Am. Soc. Mass Spectrom.* **1997**, *8*, 954.
(18) Clemmer, D. E.; Jarrold, M. F. *J. Mass Spectrom.* **1997**, *32*, 577−592.
(19) Suckau, D.; Shi, Y.; Beu, S. C.; Senko, M. W.; Quinn, J. P.; Wampler, F. M.; McLafferty, F. W. *Proc. Natl. Acad. Sci. U.S.A.* **1993**, *90*, 790.
(20) Wood, T. D.; Chorush, R. A.; Wampler, F. M.; Little, D. P.; O'Connor, P. B.; McLafferty, F. W. *Proc. Natl. Acad. Sci. U.S.A.* **1995**, *92*, 2451.
(21) McLafferty, F. W.; Guan, Z.; Haupts, U.; Wood, T. D.; Kelleher, W. L. *J. Am. Chem. Soc.* **1998**, *120*, 4732.
(22) Reimann, C. T.; Velázquez, I.; Tapia, O. *J. Phys. Chem.* **1998**, *102*, 9344.
(23) Theorell, H.; Akesson, A. *J. Am. Chem. Soc.* **1941**, *63*, 1818.
(24) Robinson, J. B., Jr.; Strottmann, J. M.; Stellwagen, E. *J. Biol. Chem.* **1983**, *258*, 6772.
(25) Myer, Y. P.; Saturno, A. F. *J. Protein Chem.* **1991**, *5*, 481.
(26) Goto, Y.; Nishikiori, S. *J. Mol. Biol.* **1991**, *222*, 679.
(27) Tsong, T. Y. *Biochem.* **1973**, *12*, 2209.
(28) Dyson, H. J.; Beattie, J. K. *J. Biol. Chem.* **1982**, *257*, 2267.
(29) Pryse, K. M.; Bruckman, T. G.; Maxfield, B. W.; Elson, E. L. *Biochemistry* **1992**, *31*, 5127.
(30) Ohgushi, M.; Wada, A. *FEBS Lett.* **1983**, *164*, 21.
(31) Kolafa, J. Unpublished (http://www.icpf.cas.cz/jiri).
(32) Brooks, B. R.; Bruccoleri, R. E.; Olafson, B. D.; States, D. J.; Swaminathan, S.; Karplus, M. *J. Comput. Chem.* **1983**, *2*, 187.
(33) Van Gunsteren, W. F.; Berendsen, H. J. C. *Mol. Phys.* **1977**, *34*, 1311.
(34) Schnier, P. D.; Gross, D. S.; Williams, E. R. *J. Am. Chem. Soc.* **1995**, *117*, 6747.
(35) Bushnell, G. W.; Louie, G. V.; Brayer, G. D. *J. Mol. Biol.* **1990**, *214*, 585.
(36) Shvartsberg, A. A.; Jarrold, M. F. *Chem. Phys. Lett.* **1996**, *261*, 86.
(37) Mesleh, M. F.; Hunter, J. M.; Shvartsberg. A. A.; Schatz, G. C.; Jarrold, M. F. *J. Phys. Chem.* **1996**, *100*, 16028.
(38) Alonso, D. O. V.; Daggett, V. *Protein Sci.* **1998**, *7*, 860.